Relative Information in Phase of Radar Range Profiles

Brian Rigling , Lee C. Potter and Randolph L. Moses

The Ohio State University
Department of Electrical and Computer Engineering
2015 Neil Avenue, Columbus OH 43210-1272 USA

ABSTRACT

In this paper, the phase of a radar range profile is shown to contain valuable information for inverse scattering problems. A physics-based high-frequency parametric model is adopted for the radar backscatter, and information is quantified using the variance of parameters estimated from noisy radar range profiles. Through analysis of the Fisher information matrix, phase is observed to yield up to a factor of ten increase in achievable resolution; moreover, phase is shown to allow reliable discrimination of frequency-dependent scattering behaviors. Results are confirmed using measured radar imagery from a 2-inch resolution X-band system.

Keywords: inverse scattering, parameter estimation, synthetic aperture radar imaging

1. INTRODUCTION

Advances in technology have steadily increased radar fractional band width, defined as band width divided by center frequency. Consequently, a point-scattering theory, while an excellent approximation for narrow band systems, has become a tenuous assumption for systems with high percent band width. Therefore, signal processing and image analysis techniques based on point-targets fail to provide the full inference available from wide band scattering measurements.

In this paper, we attempt to address the question, "what information is available in the phase of a radar range line?" This question is posed by Rihaczek,[1] who reported a factor of two loss in functional resolution by discarding range line phase. This observation presented a "conflict with conventional thinking"[1]– namely, that after coherently computing the Fourier transform of a phase history, the phase of the range line is a noninformative nuisance parameter. We further investigate the information in phase. Our approach is to adopt an electromagnetic model for linear phase scattering mechanisms and estimate model parameters from a noisy range line or synthetic aperture radar (SAR) image. An estimation theoretic approach using Fisher's information matrix[2] provides a quantifiable measure of information loss. Further, the probabilistic approach allows analysis of the effect of noise.

1.1. A Physical Scattering Model

In this paper we focus on phase information as a function of radar fractional band width; thus, we consider down-range resolution only. The results apply to high range resolution real aperture radar with simple extension to SAR imagery. We adopt an electromagnetic scattering model based on the geometric theory of diffraction[3,4] to write a radar phase history as a superposition of linear phase scattering terms

$$S(f) = \sum_i A_i \left(\frac{jf}{f_c}\right)^{\alpha_i} \exp\left\{-j\frac{4\pi f}{c}x_i\right\} + n(f) \tag{1}$$

where c is the propagation speed, f_c is the center frequency, and $n(f)$ is an additive complex white Gaussian noise process with variance σ^2. A two-dimensional extension to SAR data is given by Gerry *et al.*[5] In Equation (1), x_i is the location of the target phase center relative to a phase reference point, and the parameter α_i characterizes frequency dependence. Example values of α are given in Table 1 for canonical target geometries. Values of α less than zero correspond to diffraction, $\alpha = 0$ characterizes an ideal point target, $\alpha = 0.5$ characterizes a singly curved surface, such as a tophat, and $\alpha = 1$ characterizes flat plate scattering, such as from a trihedral corner reflector.

The amplitude parameter A_i in Equation (1) is real-valued for a perfect electrical conductor (PEC) and is well-approximated as real-valued for dielectric layers above PEC, provided the layer is a small fraction of c/f_c.[6]

Send correspondence to L.C.P., potter.36@osu.edu

1.2. On the Point-Scattering Assumption

The physical model in Equation (1) provides insight to the applicability of a point scattering assumption for a narrow band radar system. Consider, for example, $f_c = 30\,\text{GHz}$ and 1 meter Rayleigh resolution (150 MHz). The $1\,\text{m}^2$ image resolution cell may contain many scattering objects, which leads to a behavior well-approximated by a pixel value with random phase[10] (and a beta distribution on pixel amplitude). Further, for the 0.5% factional band width,

$$|f^0| \approx |f^\alpha| \tag{2}$$

for $\alpha \in (-1, 1)$; this approximation is quantified by Chiang.[7–9] Thus, a point scattering model with uniform random phase is a justifiable assumption for data processing in this narrow band case. Indeed, the peak of the Fourier transform yields the maximum likelihood (ML) estimate for the location of a single, random phase target.[11]

In contrast, with increasing band width and fixed center frequency, the $\alpha = 0$ point target approximation becomes increasingly worse for frequency dependent responses, and the number of scattering targets in a Rayleigh resolution cell decreases.

1.3. A Measure of Information

We seek to characterize the information about the parameter vector $\{A, \alpha, x\}$ carried in the range profile phase. Bruzzone and Kaveh[12] offer a measure of relative information, R

$$R = \frac{|M|}{|I|} \tag{3}$$

where $|I|$ is the determinant of Fisher's information for the parameters given the complex data and $|M|$ is the determinant of Fisher's information for the parameters given only the magnitude. The inverse of the Fisher's information matrix gives the Cramér-Rao lower bound (CRLB) for the error covariance of any unbiased parameter estimator.[2] Therefore, $R = |I^{-1}|/|M^{-1}|$, and we choose to report relative information by comparing parameter estimation error variances. More generally, location estimation variance provides a principled definition of radar resolution.[5,13]

The phase of a signal contains no useful information if it can be recovered uniquely from the signal magnitude via nonparametric techniques. In the absence of noise, the phase of a maximum phase signal is uniquely recoverable, up to $\pm\pi$, from the magnitude of the transform.[14] The signal model in Equation (1) is maximum phase for $\alpha \geq 0$; however, in the inevitable presence of measurement noise, the sampled signal $S(f)$ is not maximum phase, and the signal cannot be perfectly recovered.

2. ANALYSIS OF ESTIMATION VARIANCE

To effectively measure the information in the complex-valued range profile and its magnitude, in relation to the scattering model parameters, we construct three curves as functions of signal-to-noise ratio (SNR) and band width. These curves are: (1) the CRLB using the complex data, (2) the parameter error variances obtained using maximum likelihood (ML) estimation with the complex data, and (3) the observed parameter error variances obtained from estimation using the magnitude data. We define

$$\text{SNR} = 10 \log_{10} \left(\frac{E}{\sigma^2} \right) \tag{4}$$

Table 1. Alpha values for canonical scatterers.

α	Example scattering geometries
1	flat plate at broadside; dihedral; trihedral
0.5	singly curved surface reflection; tophat
0	point; sphere; straight edge specular
-0.5	edge diffraction
-1	corner diffraction

where E is the average energy of the N frequency domain samples of the backscattered signal and σ^2 is the noise variance from Equation (1). This definition of SNR is related to the commonly used peak-to-noise ratio (PSNR) in the range profile by $\text{PSNR} = \text{SNR} + 10\log_{10} N$. Note that N increases with band width, if the frequency sample spacing, and hence unambiguous range, are held constant. An unwindowed discrete Fourier transform (DFT), with zero padding, is used to obtain a range profile from the phase history samples.

2.1. A Variance Bound Using Complex Data

The CRLB provides a lower bound on the estimation error variance for any unbiased estimator. The CRLB is given by the inverse of the Fisher's information matrix[2]

$$I_{ij} = \mathcal{E}\left\{\left(\frac{\partial \log p(S|\theta_i)}{\partial\theta}\right)^H \left(\frac{\partial \log p(S|\theta_j)}{\partial\theta}\right)\right\} \tag{5}$$

where $\log p(S|\theta_i)$ is the log-likelihood function of the sampled data S given the parameter vector element θ_i. For the scattering model in Equation (1), $\theta = \{A, x, \alpha\}$, and each element of the 3×3 matrix I is a function of θ, σ^2, f_c, and band width. The second and third diagonal elements of I^{-1} lower bound the error variances for x and α, respectively. Derivation of the CRLB for the model in Equation (1) is straightforward.[15,8]

2.2. Maximum Likelihood Estimation

We estimate the error variances for estimated x and α using Monte Carlo simulation. Given θ, f_c, band width and N, a simulated radar phase history is computed from Equation (1). An X-band center frequency, $f_c = 10\,\text{GHz}$, is used in all cases reported. For each trial, noise of variance σ^2 is added, and a ML estimate is computed for θ. In each trial, the location parameter x is randomly selected, with uniform distribution over a range gate, to remove any dependence on the target location within the time-domain sampling interval. Two sets of trials are conducted. First, $\alpha = 1$ is assumed known, and x is estimated. Second, both x and α are randomly chosen, where α is equally likely from $\{0, 0.5, 1\}$; the model parameters are then estimated from the noisy complex-valued range lines. For each choice of band width and SNR, parameter estimation variance is averaged from 1000 trials.

2.3. Estimation Variance with Phase Discarded

To evaluate the efficacy of signal analysis when the range line phase is discarded, we again estimate error variances via Monte Carlo simulation. The experiment design follows the complex-valued data study in Section 2.2, except that the noisy range lines are replaced by their magnitudes. The resulting N data points, without zero padding, have an uncorrelated Rician joint probability density given by

$$f_v(v) = \frac{v}{\sigma^2}\exp\{-\sigma^2(v^2 + \bar{v}^2)/2\} I_0\left(\frac{v\bar{v}}{\sigma^2}\right) \tag{6}$$

where σ^2 is the noise variance in the complex sample, $\bar{v}$ is the mean of the magnitude sample, and I_0 is the zeroth-order modified Bessel function of the first kind. Zero padding yields correlated samples.

The density in Equation (6) apparently makes evaluation of the CRLB intractable. In addition, the numerical instability of the ML estimator prompts the use of a non-linear least-squares (NLLS) estimator instead. Asymptotically, errors for the NLLS estimator converge in probability to the ML estimation error distribution.[16]

3. SIMULATION RESULTS

The results of three performance simulations discussed in Section 2 are presented in Figures 1, 2 and 3, shown as mean absolute error (MAE) versus SNR. In all cases, the ML estimates lie very close to the CRLB for the complex-valued data, indicating that the estimates are nearly efficient. For estimation errors using magnitude only, results are shown for zero padding to length $1.5N$; less zero padding impairs estimation performance and additional zero padding does not significantly improve estimation performance.

In Figure 1, the frequency dependence, α, is assumed known; the amplitude and location are estimated. The curves show that discarding phase spoils achievable resolution by over a factor of 10.

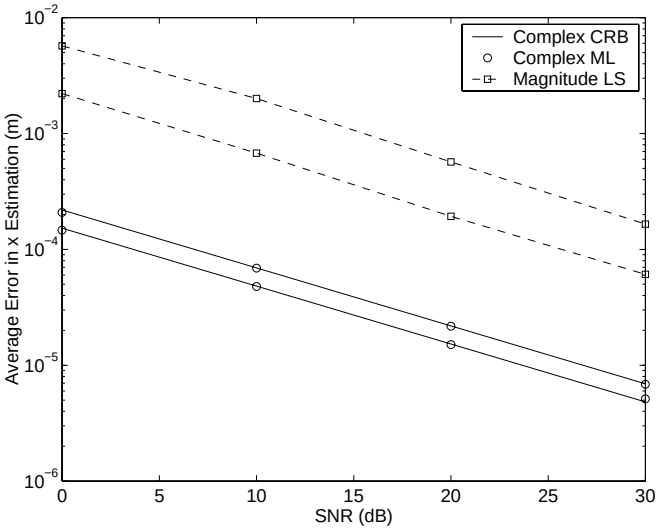

Figure 1. Average x estimation error curves for 4 inch (upper) and 2 inch (lower) Rayleigh resolution, with known α and $1.5N$ DFT oversampling.

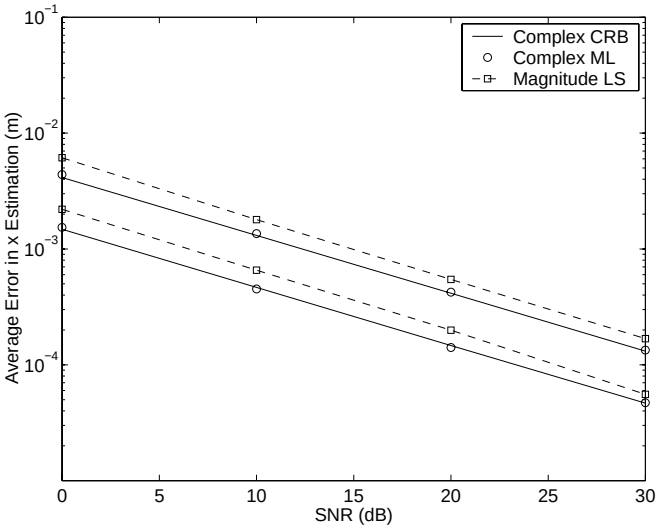

Figure 2. Average x estimation error curves for 4 inch (upper) and 2 inch (lower) Rayleigh resolution, with unknown α and $1.5N$ DFT oversampling.

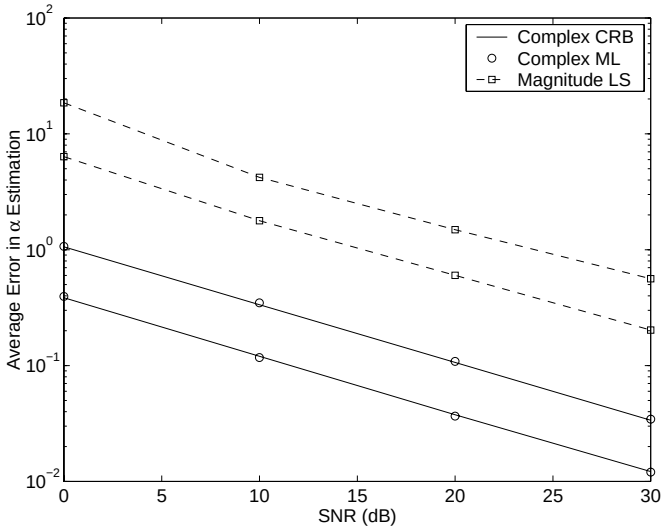

Figure 3. Average α estimation error curves for 4 inch (upper) and 2 inch (lower) Rayleigh resolution, with unknown x and $1.5N$ DFT oversampling.

In Figure 2, α is unknown and the triple $\{A, x, \alpha\}$ is estimated. We observe that absence of prior knowledge of α lessens this resolution gap; here, the resolution loss by discarding the phase is less than a factor of two. Retention of the phase provides the resolution gain equivalent to approximately 2 dB improvement in SNR.

The relative information between magnitude profiles and complex-valued range profiles is more striking in Figure 3, where the mean absolute error is shown for α estimates. In the curve, consider a SNR of 10 dB and a 3 GHz band width, corresponding to 5 cm (2 inch) Rayleigh resolution. We observe a mean absolute error of approximately 0.1 using the phase information, in contrast to a MAE of 2.0 when the phase is discarded. Given a physical range of $[0, 1]$ for nondiffractive scattering, the loss of phase renders the frequency dependence unobservable from the noisy data. Indeed, even a 30 dB SNR level yields a MAE of 0.2 when phase is discarded. In summary, accurate estimation of frequency dependence, α, requires either large fractional band width or high SNR, and loss of phase leaves α inaccessible when processing data from existing radar systems.

4. INTUITIVE VIEW

An intuitive explanation can be offered for the increased error in estimating α without phase. Figure 4a shows the magnitude profiles for $\alpha = \{0, 0.5, 1\}$, and Figure 4b shows the phase profiles for the same selection of α values. Under noiseless conditions, the magnitude profiles are extremely similar, making them virtually indistinguishable in the presence of noise. However, significant differences show in the phase profiles. These differences are due to the j^{α} term in Equation (1).

5. MEASURED SAR DATA

In this section, we analyze measured SAR data to test the performance trends predicted by simulation. Complex-valued spotlight SAR images of 40 trihedrals and 40 tophats are taken from the Grayling, Michigan Ultra-fine resolution SAR (GUS) data collection. The 3 GHz band width of the X-band system provides 5 cm Rayleigh resolution. From each image, we extract a down-range profile through the target. Estimation performance is investigated by constructing histograms of estimates for frequency parameter, α, and of estimation errors for the location parameter, x.

For estimation of α, we calibrate a 2-3 dB variation in antenna gain[17] and an unspecified side lobe windowing by normalizing trihedral phase histories by the mean magnitude of observed top hat responses. From Table 1, the predicted frequency dependence of the normalized trihedral signatures is therefore $f^1/f^{0.5} = f^{0.5}$. In Figure 5

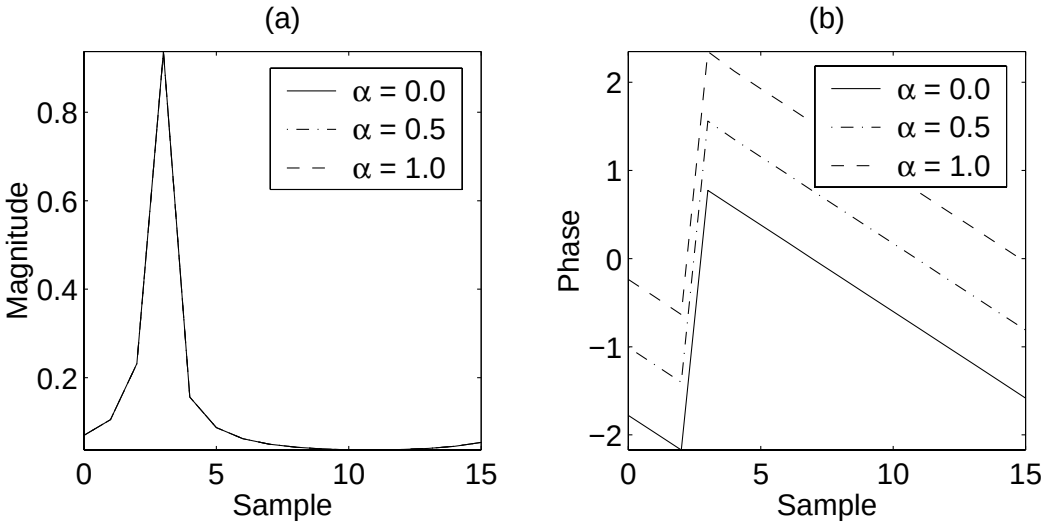

Figure 4. The effect of the α frequency dependence parameter is seen primarily in the phase of the range profile.

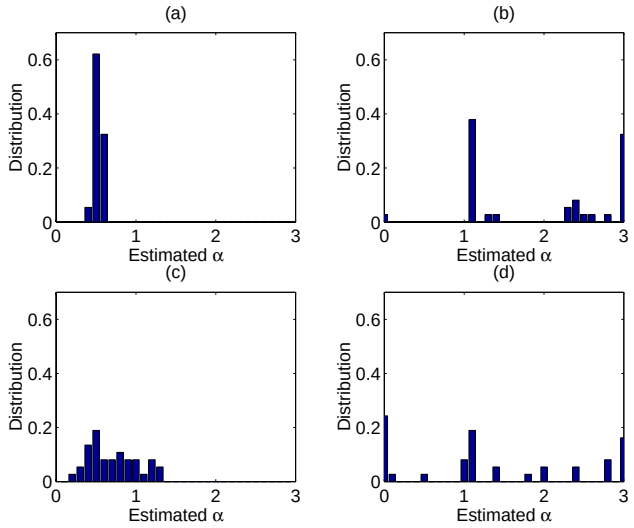

Figure 5. Estimation of α from GUS range profiles at 2-inch resolution, using the complex profile yields α estimates which allow discrimination of scattering frequency dependence, but using the magnitude does not. (a) 2-inch complex, (b) 2-inch magnitude, (c) 4-inch complex, (d) 4-inch magnitude.

estimation results using the 40 normalized trihedral signatures are shown for four cases. In Figure 5a, α is estimated from the 2 inch resolution phase history (using magnitude only of the frequency samples, owing to the lack of antenna phase calibration). The frequency dependence is correctly identified for all 40 trihedrals; the mean absolute error is only 0.05. In Figure 5c, the resolution is spoiled to 4 inches. Estimation accuracy is degraded, as expected, but nonetheless provides a 0.37 standard error – less than the 0.5 difference distinguishing flat surfaces from singly curved targets. Figure 6a and 6c are computed from the magnitude only of the phase histories and are therefore conservative predictors of estimation performance possible if the calibrated complex range lines were available.

In contrast, Figures 5b and 5d show, for the 2 inch and 4 inch data sets, histograms of estimated α parameters when phase is discarded from the range profiles. Here, only 1 of 80 image chips is correctly identified as containing

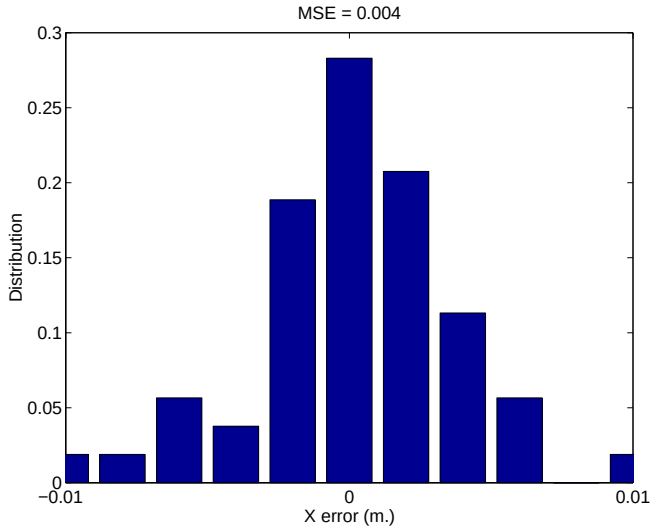

Figure 6. Relative error in estimating x with GUS magnitude range profiles at 2-inch resolution.

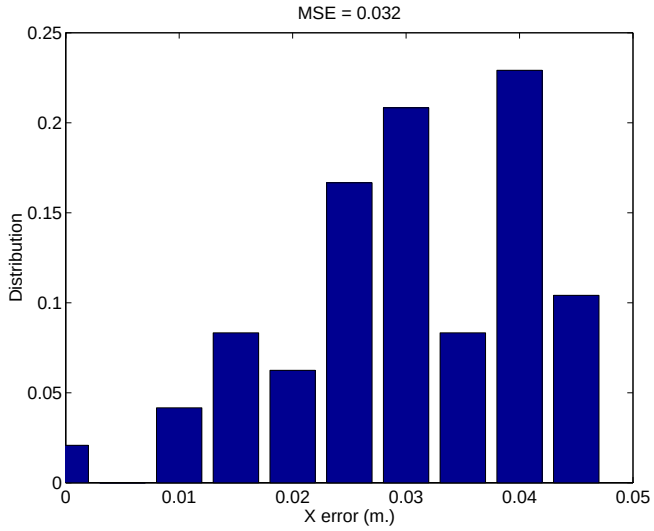

Figure 7. Relative error in estimating x with GUS complex range profiles at 4-inch resolution.

a target with $f^{0.5}$ frequency dependence. Thus, the importance of phase in the range line data is strongly confirmed by this one limited empirical study.

Next, we consider the accuracy of location estimates. In the absence of ground truth, we use the 2 inch resolution complex data to estimate nominal locations, and for lesser band width or magnitude data sets report location variance relative to these nominal values. Figure 6 shows the distribution of relative location errors using 2 inch resolution magnitude only range profiles. Figure 7 shows the distribution of relative location errors using 4 inch resolution complex range profiles. The ratio of the two MSE values is approximately 8.0 in agreement with the performance prediction in Figure 2.

6. CONCLUSIONS

In SAR images and range profiles, the phase is informative. Fisher's information, combined with physical scattering models, provides a method to quantify and predict the information carried by the phase. Further, estimation accuracy provides a useful definition of radar resolution, incorporating scattering behavior, band width, and SNR. For targets of unknown frequency dependence, the range profile phase provides the equivalent of 2 dB improvement in the phase history SNR and over 10 times resolution improvement if the target frequency response is known. More strikingly, the phase information makes possible the estimation of frequency dependence. These theoretical predictions are confirmed in measured X-band SAR imagery.

The conclusions presented here assume a stationary phase center for a PEC target, and hence linear phase responses in the frequency domain. Rihaczek and Hershkowitz[18] postulate an empirically motivated cubic phase scattering model and demonstrate the essential role of image phase in the associated parameter estimation task. Alternatively, electromagnetic modeling of scattering mechanisms on man-made targets[15] can be used in conjunction with parameter estimation to detect and analyze image features arising from multi-bounce and other non-linear phase mechanisms not adequately addressed by the conventional point-target processing methods.

ACKNOWLEDGMENTS

The authors thank Dr. Robert Hummel of the Defense Advanced Research Projects Agency and Dr. John Gorman of Veridian-ERIM International for access to the Grayling ultra-fine resolution SAR imagery. This work was sponsored by the US Air Force Materiel Command under contract F33615-97-1020. The views and conclusions contained herein are those of the authors and should not be interpreted as necessarily representing the official policies or endorsements, either expressed or implied, of the Air Force Research Laboratory or the US Government.

REFERENCES

1. A. W. Rihaczek, "Radar resolution of ideal point scatterers," *IEEE Trans. Aerospace and Electronic Systems*, **32**, 842–845, 1996.
2. H.L. Van Trees, *Detection, Estimation, and Modulation Theory Part I.* New York, NY: Wiley, 1968.
3. J. B. Keller, "Geometrical theory of diffraction," *J. Opt. Soc. Am.*, **52**, 116–130, 1962.
4. L.C. Potter, D.-M. Chiang, R. Carriere and M.J. Gerry, "A GTD-based parametric model for radar scattering," *IEEE Trans. Antennas Propagation*, **43**, 1058–1067, 1995.
5. M. J. Gerry, L. C. Potter, I. J. Gupta, and A. van der Merwe, "A parametric model for synthetic aperture radar measurements, *IEEE Trans. Antennas and Propagation*, **47**, 1179–1188, 1999.
6. C. A. Balanis, *Advanced Engineering Electromagnetics.* New York, NY: Wiley, 1989.
7. L. C. Potter and R. L. Moses, "Attributed scattering centers for SAR ATR," *IEEE Trans. Image Processing*, **6**, 79–91, 1997.
8. Da-Ming Chiang, *Parametric Signal Processing Techniques for Model Mismatch and Mixed Parameter Estimation.* PhD dissertation, The Ohio State University, Columbus OH, 1995.
9. M. L. Walker and J. W. Helton, "Application of signal subspace algorithms to scattered geometric optics and edge-diffracted signals," *IEEE Trans. Signal Processing*, **42**, 2217–2226, 1994.
10. David C. Munson and Jorge L. C. Sanz, "Image reconstruction from frequency-offset Fourier data," *Proc. IEEE*, **72**, 661-669, 1984.
11. Steven M. Kay, *Modern Spectral Estimation: Theory and Application*, Prentice Hall, Englewood Cliffs, 1988.
12. S. P. Bruzzone and M. Kaveh, "Criterion for selecting information-preserving data reductions for use in the design of multiple parameter estimators," *IEEE Trans. Information Theory*, **29**, 466–470, 1983.
13. H.-C. Chiang, R. L. Moses, and L. C.Potter, "Model-Based Classification of Radar Images," to appear in *IEEE Trans. Information Theory*, 2000.
14. M. H. Hayes, J. S. Lim, and A. V. Oppenheim, "Signal reconstruction from phase and magnitude," *IEEE Trans. Acoustics, Speech, and Signal Processing*, **28**, 672–680, 1980.
15. B. Rigling, MS thesis, The Ohio State University, Columbus OH, 2000.
16. H. White, "Maximum likelihood estimation of misspecified models," *Econometrica*, **50**, 1–25, 1982.
17. John Gorman, personal correspondence, 2000.
18. A. W. Rihaczek and S. J. Hershkowitz, "Man-made target backscattering behavior: Applicability of conventional radar resolution theory," *IEEE Trans. Aerospace and Electronic Systems*, **32**, 809–824, 1996.